J. Phys. A: Math. Gen. **29** (1996) 7943–7957. Printed in the UK

Equilibrium and off-equilibrium simulations of the 4d Gaussian spin glass

Giorgio Parisi†, Federico Ricci-Tersenghi‡ and Juan J Ruiz-Lorenzo§

Dipartimento di Fisica and Infn, Università di Roma, La Sapienza, Ple A Moro 2, 00185 Roma, Italy

Received 21 June 1996

Abstract. We study the on- and off-equilibrium properties of the four-dimensional Gaussian spin glass. In the static case we determine the critical temperature and the critical exponents with more precision than in previous simulations. In the off-equilibrium case we settle the general form of the autocorrelation function, and show, for the first time, that is possible to obtain, dynamically, a value for the order parameter.

1. Introduction

At present, the problem of the full characterization of the phase transition in finite-dimensional spin glasses is still open both from the static and dynamical approaches. Our discussion is focused on the four-dimensional case (the same applies in the more physical case, the three-dimensional system).

The equilibrium (static) simulations show a very neat intersection of the Binder cumulant curves, that is a signal of a phase transition at finite temperature with an order parameter (the Edward–Anderson order parameter, that we will denote hereafter as q_{EA}). We can identify this order parameter with the position of a Dirac delta in the probability distribution of the overlap, $P(q)$. Up until now, both the spontaneous replica symmetry breaking (SRSB) theory [1, 2] and droplet theory [3] are compatible with this result. Differences concern the shape of the rest of $P(q)$. In droplet theory, $P(q)$ is the sum of two Dirac deltas, one in q_{EA} and another in the opposite overlap, and has a Binder cumulant equal to 1. The SRSB theory maintains this structure too, but adds a continuous non-zero part in the interval $(-q_{\mathrm{EA}}, q_{\mathrm{EA}})$. This is a non-trivial distribution that has a Binder cumulant different from 1, except at $T = 0$ where the SRSB theory predicts two pure states as in the droplet theory.

The main problem is the impossibility of a direct measure of the order parameter, q_{EA}. The scaling of the peak of $P(q)$ seems compatible both with a Kosterlitz–Thouless (KT) transition, i.e. $q_{\mathrm{peak}} \sim 1/L^{\alpha}$, and with a scaling $q_{\mathrm{peak}} = q_{\mathrm{EA}} + a/L^{\rho}$. Obviously the KT scenario goes against the intersection of the Binder cumulant curves. A possible explanation of this phenomena could be that the term a/L^{ρ} is bigger than q_{EA} for the range of lattice sizes that has been simulated and hence the latter is unobservable. Simulation of bigger lattices should be done in order to get $q_{\mathrm{EA}} \gg a/L^{\rho}$.

† E-mail address: parisi@roma1.infn.it
‡ E-mail address: ricci@chimera.roma1.infn.it
§ E-mail address: ruiz@chimera.roma1.infn.it

0305-4470/96/247943+15$19.50

The dynamical approach [4] has the same problems as the previously discussed static case. The main physical quantity in this approach is the spin–spin autocorrelation, defined as

$$C(t, t_w) = \frac{1}{N} \sum_{i=1}^{N} \overline{\langle \sigma_i(t_w)\sigma_i(t_w + t)\rangle}. \tag{1}$$

Usually in the literature [5] one finds the empirical formula

$$C(t, t_w) = t^{-x} f(t/t_w) \tag{2}$$

for instance in the mean filed case [6] and in the three-dimensional case [7]†.

The static limit (on-equilibrium situation) is achieved by sending t_w to infinity first, and then simulating larger t. The formula (2) for the spin–spin autocorrelation function goes to zero in this limit. However, in the case of a non-zero-order parameter, this autocorrelation function must go to q_{EA}. It is clear that in the regime of $t_w \gg t \gg 1$ there should be found a formula like

$$C(t, t_w) = (q_{EA}/f(0) + at^{-x}) f(t/t_w) \tag{3}$$

but a very long numerical simulation is needed in order to observe both the terms q_{EA} and at^{-x}. In the present work we show numerical evidence of this kind of behaviour for the first time.

Up until now, the only numerical studies of off-equilibrium dynamics in a finite-dimensional spin-glass are those of Rieger [7] in the three-dimensional case.

The four-dimensional case seems easier to simulate, since it is far away from the lower critical dimension of the spin-glasses ($d_l < 3$ [9, 10]) and the static case is thus very clear. In this paper we will mainly study the off-equilibrium dynamics of this model in order to make a comparison with the three-dimensional results by Rieger and to examine the possibility of extracting finite value for the order parameter. In addition, simulations have been performed in the static (on-equilibrium) case in order to characterize with higher precision the location of the critical temperature and the critical exponents.

Both for the off- and on-equilibrium cases we review the numerical results from the point of view of the previous discussion and we try to link both approaches in order to obtain a conclusion regarding the existence of a finite temperature phase transition, with a non-zero-order parameter.

2. Model, simulation and static observables

We have studied the 4*d* Ising spin glass with nearest-neighbour interactions and zero external magnetic field, whose Hamiltonian is

$$\mathcal{H} = -\sum_{\langle i,j\rangle} J_{ij}\sigma_i\sigma_j \tag{4}$$

where $\langle i, j\rangle$ denotes nearest-neighbour pairs and the couplings are extracted from a Gaussian distribution with zero mean and unit variance.

The static and dynamical behaviour of the model have been investigated by several different simulations during which many different observables have been measured. In this section we describe the way we have performed measurements of the static exponents and the critical temperature with a precision higher than that available in the literature [11, 12].

† Also in an on-equilibrium numerical simulation in the three-dimensional case [8], $C(t) \sim t^{-x}$.

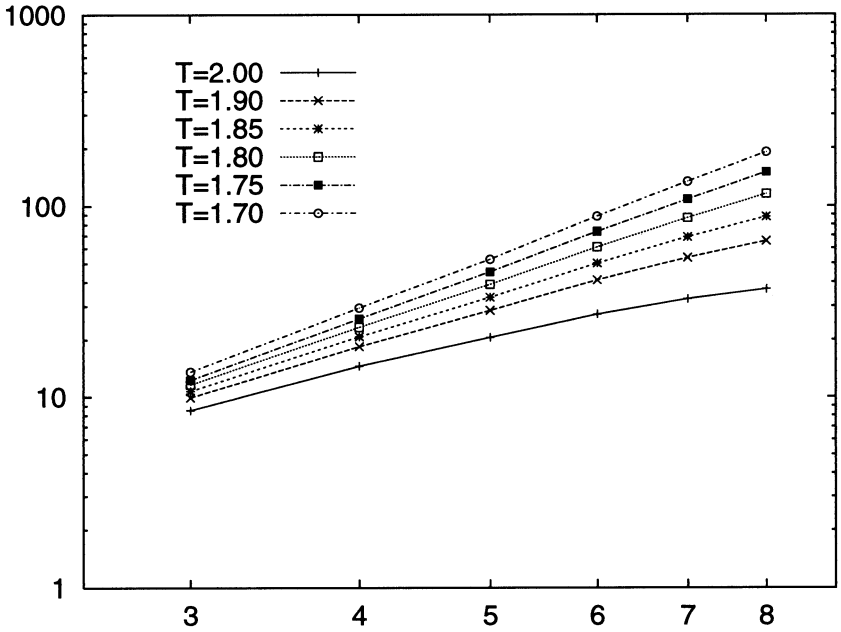

Figure 1. $\chi_{SG}(L, T)$ against L; the errors are of the order of the symbol.

The equilibrium simulations have been performed on small lattices ($L = 3$–8) to ensure the system reached equilibrium. Most of the work has been performed in a range of temperatures around the critical temperature T_c. The average over the disorder has been taken on 2048 samples for all the lattice sizes. For each realization of the quenched disorder we have simulated two replicas with spin σ_i and τ_i. This has enabled us to measure the kth cumulant of the distribution of the overlaps, $q^{(k)} \equiv \int q^k P(q)\, \mathrm{d}_q$, simply by averaging the quantity $(N^{-1} \sum_i \sigma_i \tau_i)^k$ over a large number of independent configurations.

All the calculations have been performed on a *tower* of the parallel supercomputer APE100 [13], with a real performance of about 5 Gigaflops.

A detailed study has been devoted to the calculation of the number of sweeps needed to reach the equilibrium and to the estimate of the autocorrelation time at the equilibrium. This study suggests a thermalization time of about 10^5 sweeps, being sure that using this value even the biggest system at the lowest temperature will be thermalized. To verify the correctness of this value we studied the evolution of the biggest system ($L = 8$) at the lowest temperature ($T = 1.7$): we choose three replicas of the system such that having, at the starting time, two overlaps set to zero and the third one equal to one; we have followed the evolution of these overlaps averaging over a large number of disorder configurations and we have estimated the thermalization time as the time needed in order that the three overlaps converge to a single value.

Once the equilibrium has been reached, we measured how much time was needed to decorrelate the observables. Particularly, we have seen that the overlap between two replicas has a time correlation function that decreases exponentially, $C(t) \sim \exp(-t/\tau)$. This defines a characteristic time whose typical values at $T = 1.7$ are $\tau \sim 200$ for $L = 4$, $\tau \sim 1000$ for $L = 6$ and $\tau \sim 3000$ for $L = 8$. In the final simulation, after thermalization, we measured every τ sweeps the overlap between the two replicas for a time longer than the equilibration time.

We define the spin glass susceptibility as

$$\chi_{\mathrm{SG}}(L,T)=\frac{1}{N}\sum_{i,j}\overline{\langle\sigma_i\sigma_j\rangle^2}=Nq_2^{(2)} \tag{5}$$

where $N=L^4$, $\langle(\cdot\cdot)\rangle$ is the thermodynamical average and $\overline{(\cdot\cdot)}$ the mean over the disorder, and the Binder parameter as

$$g(L,T)=\frac{1}{2}\left(3-\frac{q_L^{(4)}}{(q_L^{(2)})^2}\right). \tag{6}$$

The results of our simulations are plotted in figure 1 for the spin glass susceptibility and figure 2 for the Binder cumulant.

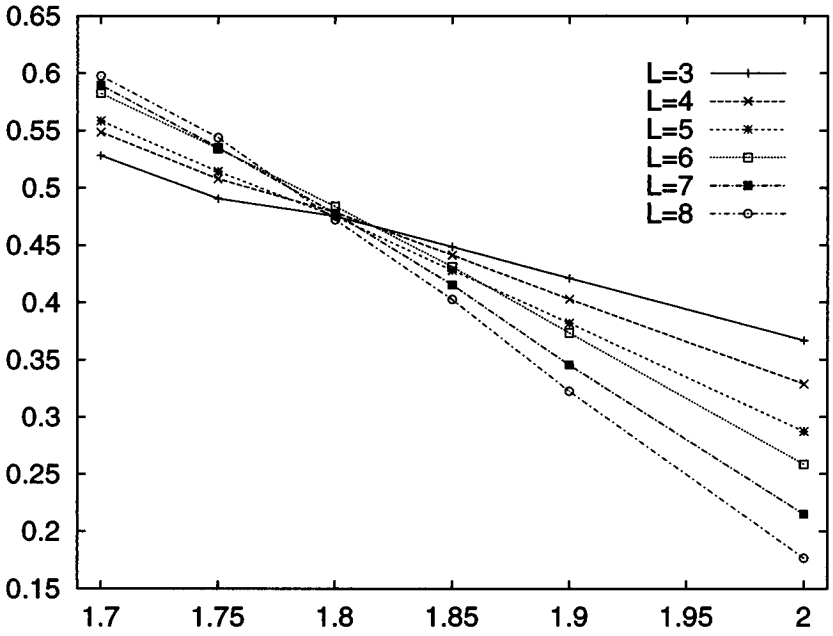

Figure 2. $g(L,T)$ against T; the errors are of the order of the symbol.

The errors on the plotted data are derived from a jackknife analysis, which also confirms that the overlaps measured every τ sweeps are decorrelated. Using finite size scaling we see that $\chi_{\mathrm{SG}}(L,T)$ and $g(L,T)$ scale as (in the scaling region)

$$\chi_{\mathrm{SG}}(L,T)=L^{2-\eta}\tilde{\chi}_{\mathrm{SG}}(L^{1/\nu}(T-T_{\mathrm{c}})) \tag{7}$$

$$g(L,T)=\tilde{g}(L^{1/\nu}(T-T_{\mathrm{c}})). \tag{8}$$

Note that at the critical temperature the Binder parameter does not depend on the size of the system, so T_{c} is the temperature where the curves of figure 2 intersect.

In the neighbourhood of T_{c} we can approximate the function $\tilde{g}$ with a linear one and obtain the following critical temperature and ν exponent:

$$T_{\mathrm{c}}=1.80\pm0.01 \tag{9}$$

$$\nu=0.9\pm0.1. \tag{10}$$

The value of ν is also confirmed by the results of the analysis performed, following [14], on the quantity

$$\left.\frac{\mathrm{d}g}{\mathrm{d}T}\right|_{T_0:g(T_0)=g_0} = \alpha L^{1/\nu} \tag{11}$$

obtaining

$$\nu = 1.06 \pm 0.06. \tag{12}$$

The prediction about the infinite volume limit of the Binder cumulant is different in the droplet theory ($g(L, T < T_c) \overset{L\to\infty}{\to} 1$) and in the SRSB picture ($g(L, T < T_c) \overset{L\to\infty}{\to} \overline{g}(T) < 1$). Unfortunately with our data ($L = 3$–8) it is impossible to extrapolate the infinite value with a precision that could discriminate, without doubt, between the two predictions.

The estimation of the anomalous dimension η can be performed by fitting the χ_{SG} data, at $T = T_c$, with a power law

$$\chi_{SG}(L, T = T_c) \propto L^{2-\eta} \tag{13}$$

obtaining $\eta = -0.35 \pm 0.05$ (the error is due mostly to the uncertainty on the critical temperature and to the rapid variation in the region around T_c of the exponent in equation (13)). These results are in agreement with those found by Bhatt and Young in [11] using a maximum size of 6^4 and 200–800 samples: $T_c = 1.75 \pm 0.05$, $\nu = 0.8 \pm 0.15$ and $\eta = -0.3 \pm 0.15$.

Using the scaling law $\gamma = \nu(2 - \eta)$ and the exponent value just calculated, we have $\gamma = 2.1 \pm 0.2$, which is in good agreement with the value obtained by the high-temperature expansions, $\gamma = 2.0 \pm 0.4$ [15].

Another series of computer runs, performed using the annealing procedure [16], let us measure the non-connected susceptibility for a wide range of temperature in the spin glass phase ($T < T_c$). We clearly see that the data diverge with increasing system sizes, even though, because of the small lattices, many different fits are possible, e.g.

$$\chi_{SG}(L, T) = A(T)L^4[1 + B(T)L^{-\Lambda(T)}] \tag{14}$$

or

$$\chi_{SG}(L, T) \propto L^{2-\eta(T)}. \tag{15}$$

Further evidence for the value of T_c can be obtained as the highest temperature where the power law fit is yet acceptable (by a χ^2 test).

3. Off-equilibrium dynamics

The second part of our study was devoted to the simulation of systems of greater dimensions (ranging from 8^4 to 32×16^3). At the beginning of every simulation the system is frozen from an infinite temperature to one in the critical region ($T \leqslant T_c$), and measurements of the autocorrelation functions immediately start with the system still out of equilibrium. Due to the huge thermalization times of the simulated systems, off-equilibrium dynamics is the most realistic situation and also the most interesting. In fact, due to the enormous number of metastable states, the dynamics is very slow and it is also reminiscent of the time passed in the spin glass phase, which we call t_w. These effects can be clearly seen by the study of the autocorrelation functions defined as

$$C(t, t_w) = \frac{1}{N}\sum_{i=1}^{N} \overline{\langle \sigma_i(t_w)\sigma_i(t_w + t)\rangle} \tag{16}$$

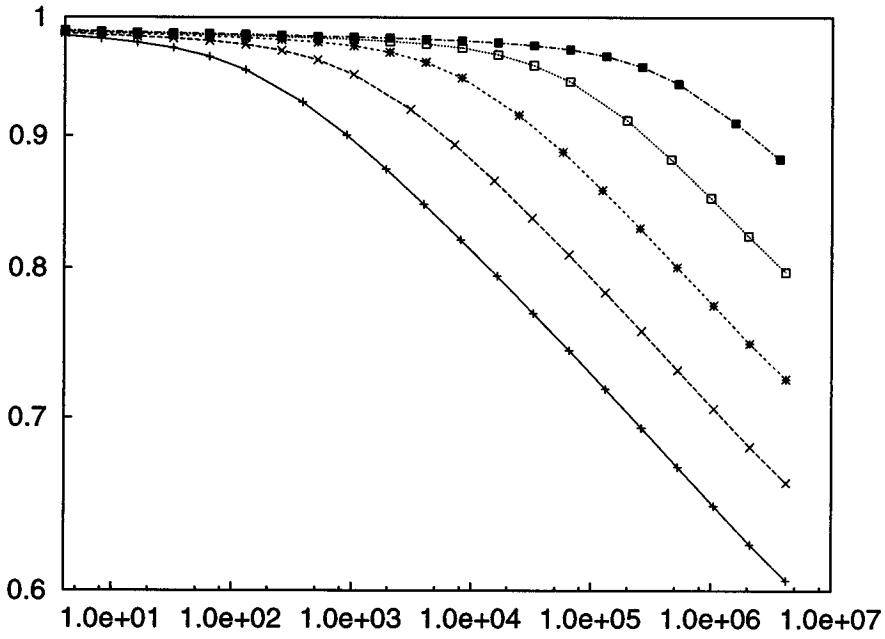

Figure 3. $C(t, t_w)$ against t at $T = 0.2$ with $t_w = 2^7, 2^{10}, 2^{13}, 2^{16}, 2^{19}$ (bottom to top).

where $\overline{(\cdot\cdot)}$ is the mean over the disorder and $\langle(\cdot\cdot)\rangle$ stands not for an average over the equilibrium thermodynamic state, since we are not at equilibrium, but for an average over the thermal histories. Nevertheless, we found that, for the system sizes we considered, disorder fluctuations are always stronger, so generally we omit the angular brackets.

Our simulations cover the cold phase (from $T = T_c = 1.8$ down to $T = 0.2$) through the set of waiting times $t_w = 2^k$ with $k = 7, 8, \ldots, 21$ and averaging over 3072 disorder realizations systems of volumes from 8^4 to 12^4.

In the four-dimensional Ising spin glass the presence of a critical temperature and the subsequent spin glass phase has been widely accepted, so the principal question that remains to be answered is which kind of phase space arises for $T < T_c$. In the literature there are principally two theories that try to describe the spin glass systems in their low temperature phase: one is based on a mean-field-like approximation which predicts a spontaneous replica symmetry breaking (SRSB picture); the other one, starting from a Migdal–Kadanoff renormalization group technique, concludes that the system remains trivial, with only one pure state (droplet model). The predictions of the two theories regarding the autocorrelation function are different: the SRSB picture predicts that in the limit of $t_w \to \infty$ the autocorrelation must be a power law that converges to the Edward–Anderson parameter (q_{EA})

$$C(t, t_w) = (q_{EA} + at^{-x}) \frac{f(t/t_w)}{f(0)} \tag{17}$$

while in the droplet model the relaxation is slower,

$$C(t, t_w) = (\log t)^{-\theta/\psi} C' \left(\frac{\log(t/\tau)}{\log(t_w/\tau)} \right). \tag{18}$$

The data we collected (see figures 3 and 4) seem to agree with the scaling law used in [7] and in [6]

$$C(t, t_w) = t^{-x'(T)} \tilde{C}(t/t_w) \tag{19}$$

with a scaling function

$$\tilde{C}(z) = \begin{cases} \text{constant} & \text{for } z \to 0 \\ z^{x'(T)-\lambda(T)} & \text{for } z \to \infty. \end{cases} \tag{20}$$

The values of the exponent $x'(T)$ are shown together with the values of $x(T)$ in figure 9, while $\lambda(T)$ is shown in figure 7 (later).

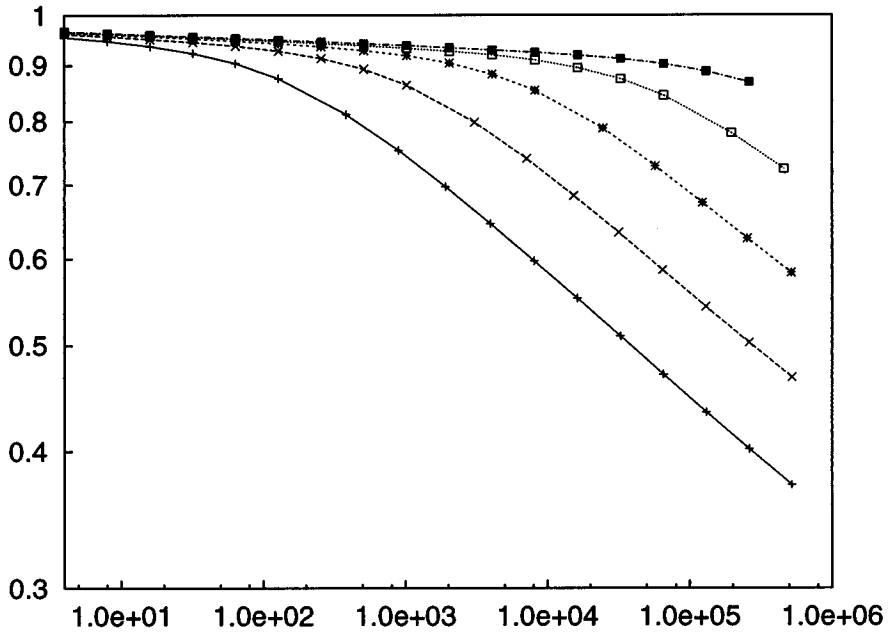

Figure 4. $C(t, t_w)$ against t at $T = 0.45$ with $t_w = 2^7, 2^{10}, 2^{13}, 2^{16}, 2^{19}$ (bottom to top).

To evaluate the goodness of the two proposed scaling formulae equations (19) and (18) we show in figure 5 the $T = 0.45$ data rescaled with the former law, noting that they collapse very well on a single curve. In contrast, using the droplet model scaling law, it was impossible for us to find a value for the parameters θ/ψ and τ such to force the data over a single curve; in figure 6 we show the best scalings we could obtain in order to make the data collapse in the $t < t_w$ or in the $t > t_w$ region.

Nevertheless in the very good rescaling of the data in figure 5 we also performed a deeper analysis in order to find the value of the Edward–Anderson parameter, q_{EA}, which is assumed to be zero in equation (19). The value of q_{EA} can be found by performing the $t \to \infty$ limit *after* the $t_w \to \infty$ limit; for this purpose we have performed very long simulations (more than 4 million Monte Carlo sweeps). We note that the scaling laws obeyed by the data in the two regions $t \gg t_w$ and $t \ll t_w$ are essentially different. In the former the data can be fitted by a power law of the ratio t/t_w, while in the latter we obtain a law equal to that of equation (17) multiplied by a function of t/t_w which is almost a constant.

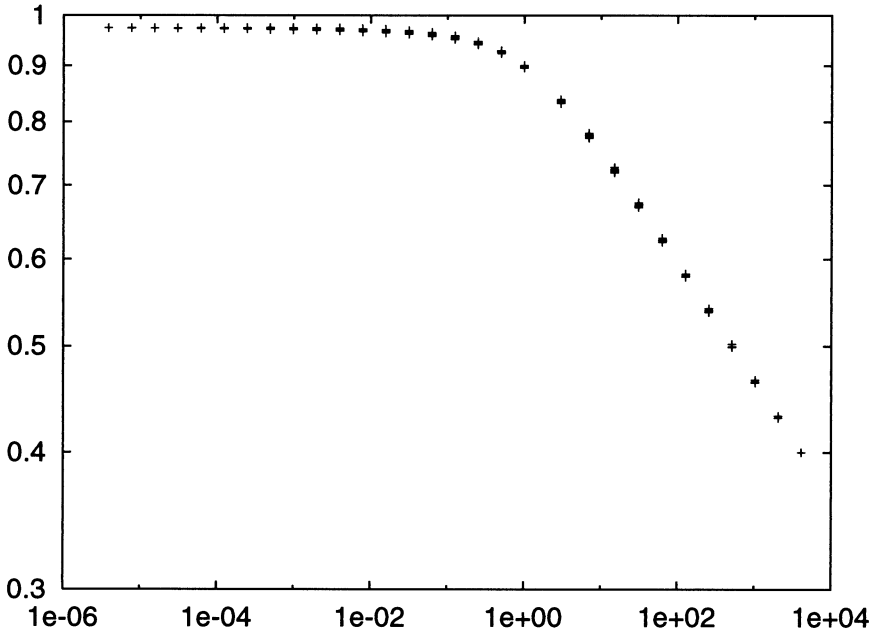

Figure 5. $T = 0.45$ aging autocorrelation function rescaled following equation (19), with $x = 0.0054$. We plot $t^x C(t, t_w)$ against t/t_w.

Such a behaviour for $C(t, t_w)$ can be justified assuming that the system evolves as long as $t \ll t_w$ with a quasi-equilibrium dynamics which converges to q_{EA}, whereas for $t \gg t_w$ it decorrelates faster and towards zero ($C \sim t^{-\lambda}$ with $\lambda(T) \gg x(T), \forall T$), but always with a critical slowing down.

The values for $\lambda(T)$ have been obtained by fitting the $C(t, t_w = 0)$ data with a power law and for $t_w \neq 0$ with

$$C(t, t_w) \propto \left(\frac{t}{t_w}\right)^{\lambda(T)} \tag{21}$$

in the range $t/t_w \geqslant 15$. In figure 7 we plot the results either for $t_w = 0$ or for $t_w \neq 0$. We note that both fits are compatible with the linear dependence on the temperature predicted form the experimental measurements [17].

In the region $t_w/t \geqslant 32$ we have performed the analysis assuming that the correlation function could be factorized as

$$C(t, t_w) = (q_{EA} + at^{-x})\bar{C}(t/t_w) \tag{22}$$

where we have approximated $\bar{C}(z) = 1 - c_1 z^{c_2}$ for $z \to 0$. First of all, the rescaling function $\bar{C}(t, t_w)$ has been calculated by fitting the correlation function at a fixed value of t. Later, once the data were divided by this function, we verified that the curves for different ratios t/t_w collapse over a single curve and we interpolated the data via a power law plus constant, following equation (17). In figure 8 we plot in a log–log scale typical $C(t, t_w)/\bar{C}(t/t_w)$ data with the best fit; we note that up until now in the literature these data have been fitted via a simple power law, while it is evident that the points in figure 8 are not on a straight line.

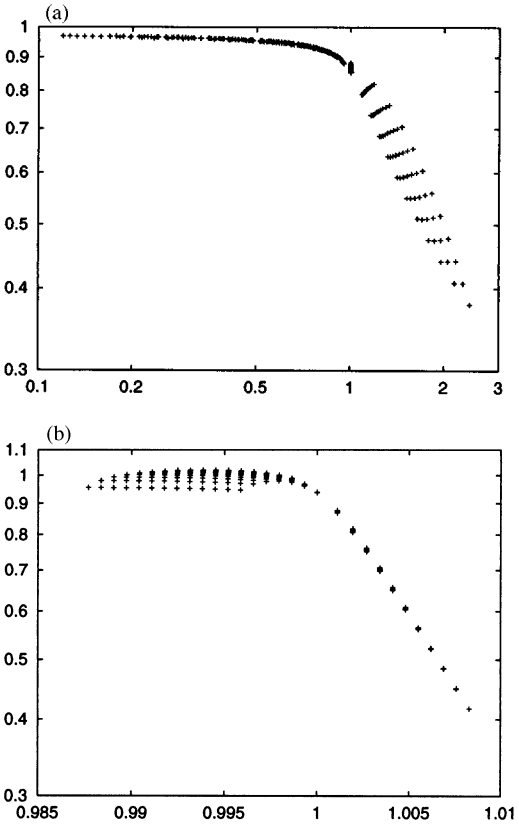

Figure 6. Tentatives of rescaling following the droplet model law equation (18): graph (a) $\theta/\psi = 0.0054$ and log $(\tau) = -1$; (b) $\theta/\psi = 0.043$ and $\log(\tau) = -1000$.

From these fits the values of q_{EA} and x as a function of the temperature (see figures 9 and 10) can be obtained. As a guide to the eye, we show in figure 10 the simpler function which behaves like $|T - T_{\mathrm{c}}|^{\beta}$ near the critical temperature and tends to 1 for $T = 0$,

$$q_{\mathrm{EA}}(T) = \left(\frac{T_{\mathrm{c}} - T}{T_{\mathrm{c}}}\right)^{\beta} \tag{23}$$

where $T_{\mathrm{c}} = 1.8$ and $\beta = (\nu/2)(d - 2 + \nu) = 0.74$ (using the values found in the previous section). From figure 9 we note that only the quantity $x(T)$, and not $x'(T)$, is such that $x(T)/T$ is roughly independent from the temperature, so that only in this parametrization the $t_{\mathrm{w}} = \infty$ autocorrelation function ($R(t; T) = C(t, t_{\mathrm{w}} = \infty)$ at temperature T) can be written as

$$R(t; T) - R(\infty; T) = b(T) \exp(-BT \log(t)). \tag{24}$$

The relevance of the variable $T \log(t)$ has been observed in experiments on magnetic remanence in a wide region [17].

We define the off-equilibrium correlation length, $\xi(t)$, as the typical distance over which the system is thermalized after a time t. For this domain growth the SRSB picture predicts a power law [9].

$$\xi(t) \propto t^{1/z(T)} \tag{25}$$

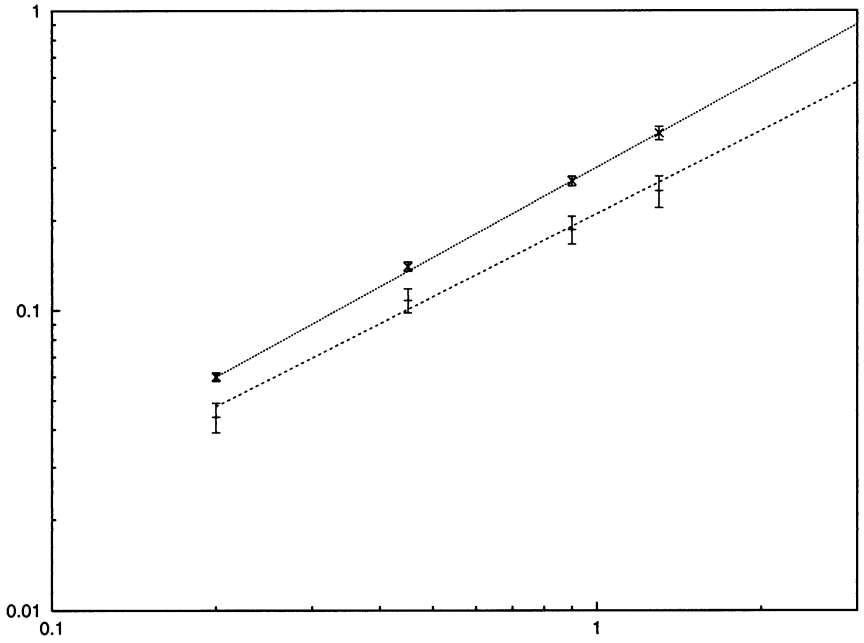

Figure 7. $\lambda_{t_w=0}(T)$ (top) and $\lambda_{t_w\neq 0}(T)$ (bottom) against T; the lower line represents the power fit $\lambda(T) = 0.21(1)T^{0.92(7)}$; the upper line both the linear and the power fit: $\lambda(T) = 0.000(3) + 0.30(1)T$ and $\lambda(T) = 0.303(8)T^{1.00(3)}$, respectively.

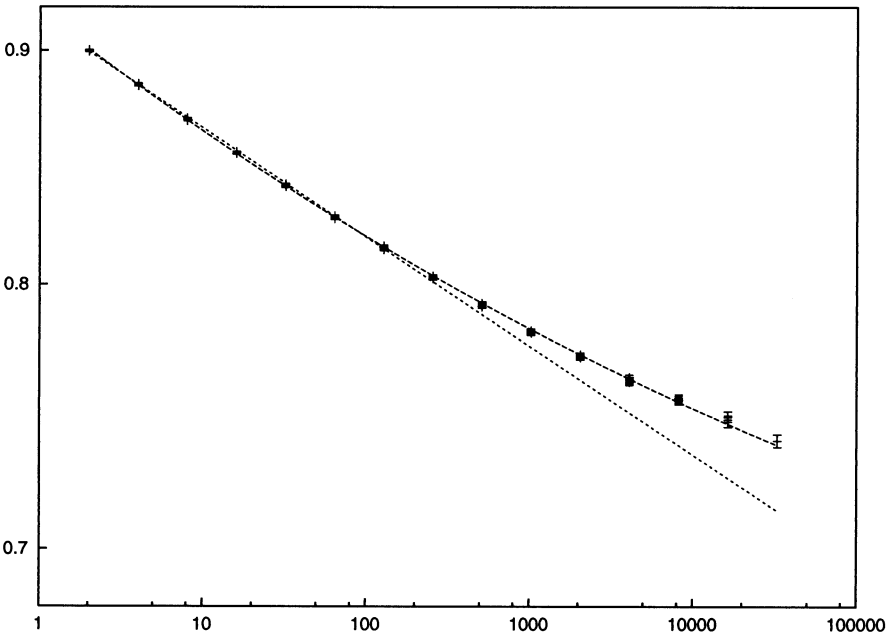

Figure 8. $C(t, t_w)/\bar{C}(t/t_w)$ data at $T = 0.9$ against t; the upper line is the best power law plus constant fit: $0.60(4) + 0.32(4)t^{-0.08(1)}$, while the lower line is the best power law fit.

while in the droplet model, where the energy barriers scale proportionally to L^{ψ}, the law is

$$\xi(t) \propto (T \log t)^{1/\psi}. \tag{26}$$

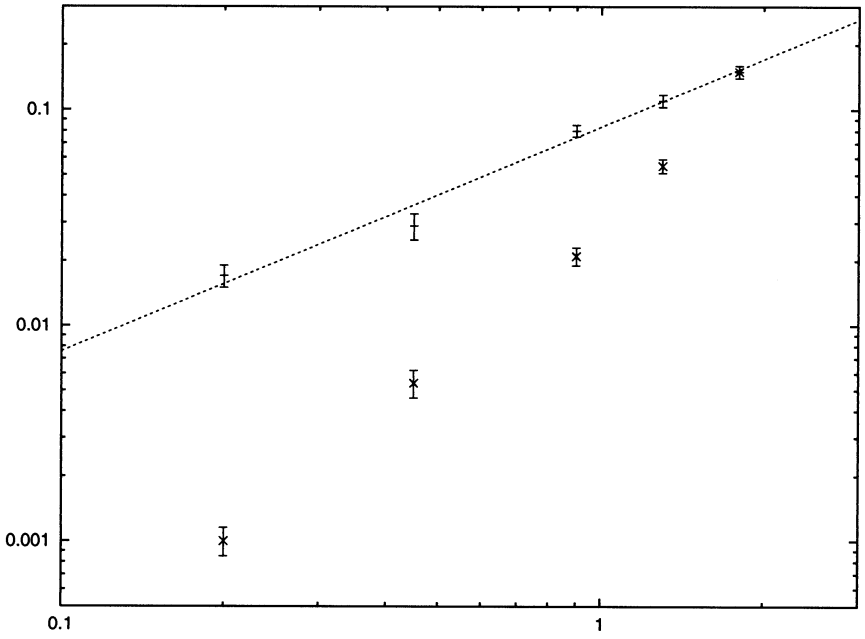

Figure 9. $x(T)$ (top) and $x'(T)$ (bottom) against T (the value at the greater temperature is equal: $x(T_c) = x'(T_c)$); the line is the best power fit $x(T) = 0.083(3)T^{1.04(7)}$.

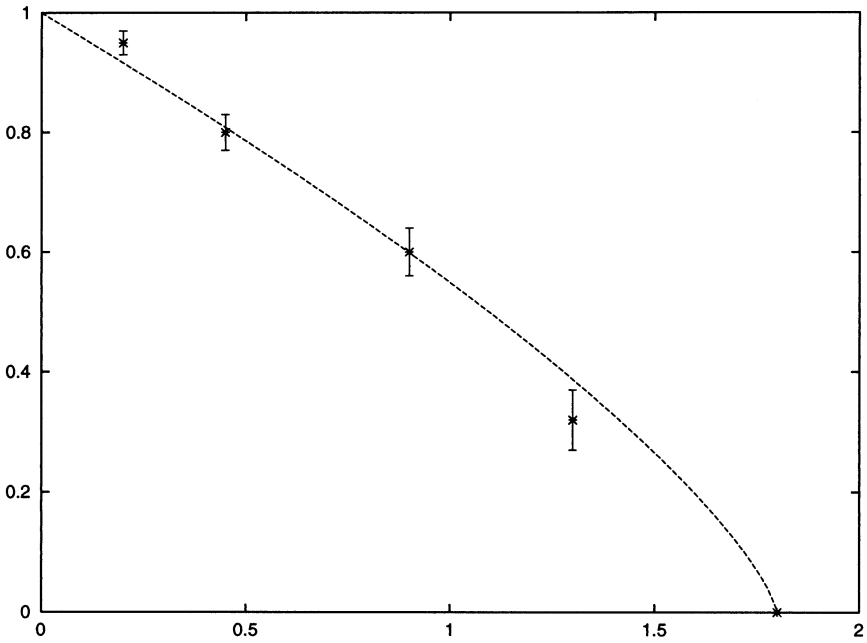

Figure 10. The Edward–Anderson order parameter against T; the line is only a guide to the eye as explained in the text

At least at the critical temperature there is a scaling relationship between the dynamical exponent $z(T_c)$ and the one which describes the dynamics in the quasi-equilibrium regime,

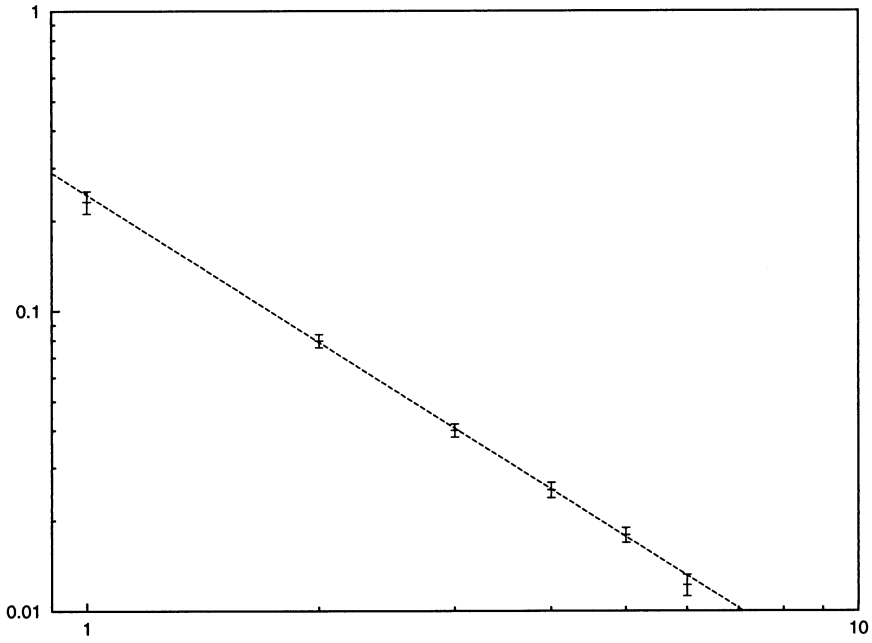

Figure 11. $G(r, t = \infty)$ against r at $T = T_c = 1.8$; the line is the power fit $0.24(1)r^{-1.63(5)}$.

$x(T_c) = x'(T_c)$ (because $q_{EA}(T = T_c) = 0$)

$$x = \frac{d - 2 + \eta}{2z}. \tag{27}$$

This equation is satisfied by all the exponents we have estimated at the critical temperature: $x = 0.15$, $\eta = -0.35$ and $z = 5.3$.

To find the behaviour of the off-equilibrium correlation length we have measured, as in [9], the equal time spatial correlation functions

$$G(r, t) = \frac{1}{N} \sum_{i=1}^{N} \overline{\langle \sigma_i(t) \sigma_{i+r}(t) \rangle^2} \tag{28}$$

where the averages are the same as in equation (16) and t is the time since the cooling. This study has been performed on systems of volume 32×16^3.

From scaling concepts we know that, at large values of r, $G(r, t)$ must behave like

$$G(r, t) \propto r^{-(d-2+\eta)} f\left(\frac{r}{\xi(t)}\right) \tag{29}$$

and, supposing $f(y) = A \exp(-By^D)$, we have fitted our data with the function

$$G(r, t) = Ar^{-(2+\eta)} \exp\left[- B\left(\frac{r}{t^{1/z}}\right)^D \right]. \tag{30}$$

In the $t \to \infty$ limit the exponential term tends to 1 and we obtain a spatial correlation function that decreases with a power law: in figure 11 we plot such a function at the critical temperature ($T_c = 1.8$). Note that from the slope of the curve we obtain an estimation of the η exponent compatible with that of section 2.

At the lower temperatures the value of η strongly depends on the r range of interpolation, because the fitting function diverges at $r = 0$. In contrast, trying to fit the data in different

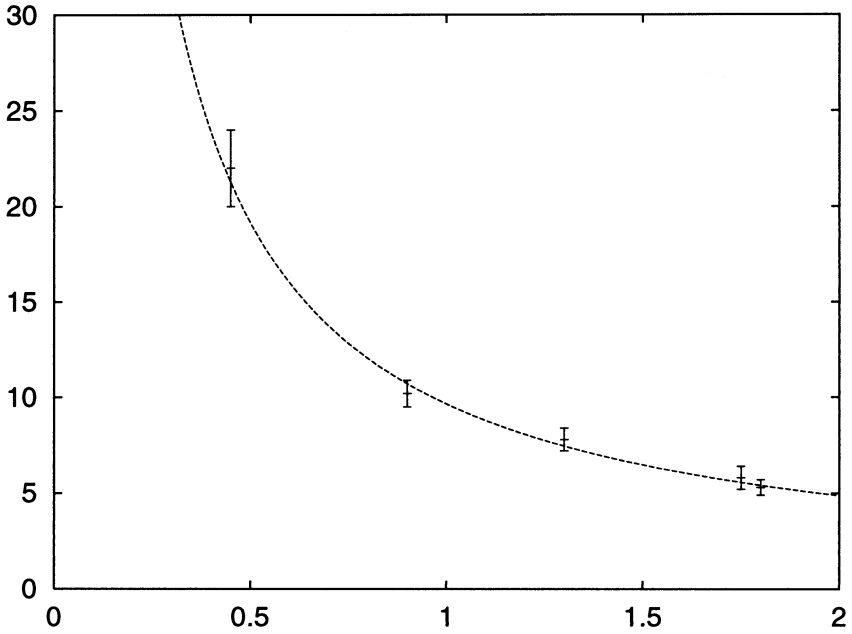

Figure 12. $z(T)$ against T; the line is the power fit, equation (31).

ranges of r, we find that the dynamical exponent $z(T)$ is a robust parameter which remains unchanged for every r range (shown in figure 12).

Fitting the plotted data with a power law we obtain, up to the critical temperature,

$$z(T) = AT^{-\alpha} \tag{31}$$

with $A = 9.7 \pm 0.5$ and $\alpha = 1.0 \pm 0.1$.

A preliminary analysis of a new set of data at $T = 0.9 = T_c/2$ suggests a value of $\eta \simeq -1$. The fact that the value of z at this temperature is higher than the corresponding value at T_c makes the evaluation of the exponent η prone to systematic error. Nevertheless this rough estimate of η is compatible with the prediction of [18].

4. Conclusions

In this paper we have studied the on- and off-equilibrium properties of the four-dimensional Gaussian spin glass.

In the static case the hypothesis of a transition following the Kosterlitz–Thouless transition has been rejected owing to the study of the on-equilibrium properties of the model: the existence of a second-order phase transition is well testified by the clean cut of the Binder cumulant curves. We have determined with more precision than in previous simulations both the critical temperature as well as the critical exponents.

In the off-equilibrium case we have settled, for the first time, a form of the autocorrelation function compatible, in the large time limits (i.e. on equilibrium), with the existence of an order parameter different from zero. We have been able to determine, in a dynamical way, the value of q_{EA} as a function of temperature (this again confirms the absence of a Kosterlitz–Thouless transition). Also we have established the temperature

dependence of the exponents that appear in these off-equilibrium dynamics, which is linear in all the cases.

The dynamics of the model seem to be described better by the SRSB theory than by the droplet theory: in effect the autocorrelation functions, properly rescaled, follow very well the power laws predicted by the former, which are quite different from the logarithmic laws predicted by the latter.

Our conclusion is that the SRSB theory seems to be, at the moment, the best picture to describe the EA model in finite dimensions greater than the lower critical dimension.

A still open problem we are planning to study in the future regards the estimate, simulating much larger lattices, of the order parameter using the static spin glass susceptibility.

Acknowledgments

We acknowledge useful discussions with E Marinari. We are very grateful to the APE group for its continuous support and valid assistance. JJR-L is supported by an EC HMC(ERBFMBICT950429) grant.

References

[1] Mézard M, Parisi G and Virasoro M A 1987 *Spin Glass Theory and Beyond* (Singapore: World Scientific)

[2] Parisi G 1979 Toward a mean field theory for spin glasses *Phys. Lett.* **73A** 203; 1980 A sequence of approximated solutions to the S–K model for spin glasses *J. Phys. A: Math. Gen.* **13** L115; 1980 The order parameter for spin glasses: a function on the interval 0-1 *J. Phys. A: Math. Gen.* **13** 1101; 1980 Magnetic properties of spin glasses in a new mean field theory *J. Phys. A: Math. Gen.* **13** 1887; 1983 Order parameter for spin-glasses *Phys. Rev. Lett.* **50** 1946

[3] Fisher D S and Huse D A 1988 Equilibrium behaviour of the spin-glass ordered phase *Phys. Rev.* B **38** 386

[4] Cugliandolo L F and Kurchan J 1994 On the out of equilibrium relaxation of the SK model *J. Phys. A: Math. Gen.* **27** 5749

[5] Rieger H 1995 Monte Carlo studies of Ising spin glasses and random field systems *Annual Review of Computational Physics II* (Singapore: World Scientific) p 295

[6] Cugliandolo L F, Kurchan J and Ritort F 1994 Evidence of aging in spin-glass meanfield models *Phys. Rev.* B **49** 6331

[7] Rieger H 1993 Non-equilibrium dynamics and aging in the three-dimensional Ising spin-glass model *J. Phys. A: Math. Gen.* **26** L615

[8] Ogielski A T 1985 Dynamics of three-dimensional Ising spin glasses in thermal equilibrium *Phys. Rev.* B **32** 7384

[9] Marinari E, Parisi G, Ritort F and Ruiz-Lorenzo J 1996 Numerical evidence for spontaneously broken replica symmetry in 3D spin glasses *Phys. Rev. Lett.* **76** 843

[10] Kawashima N and Young A P 1996 Phase transition in the three-dimensional $\pm$J Ising spin glass *Phys. Rev.* B **53** R484

[11] Bhatt R N and Young A P 1988 Numerical studies of Ising spin glasses in two, three and four dimensions *Phys. Rev.* B **37** 5606

[12] Badoni D, Ciria J C, Parisi G, Ritort F, Pech J and Ruiz-Lorenzo J J 1993 Numerical evidence of a critical line in the 4d Ising spin glass *Europhys. Lett.* **21** 495

[13] The APE collaboration 1993 The APE100 computer: the architecture *Int. J. High Speed Computing* **5** 637; 1993 The software of the APE100 processor *Int. J. Mod. Phys.* C **4** 955; 1993 A hardware implementation of the APE100 architecture *Int. J. Mod. Phys.* C **4** 969

[14] Iniguez D, Parisi G and Ruiz-Lorenzo J J 1996 Simulation of 3-d Ising spin glass model using three replicas: study of Binder cumulants *Preprint* cond-mat/9603083 *J. Phys. A: Math. Gen.* to appear

[15] Singh R R P and Chakravarty S 1986 Critical behaviour of an Ising spin-glass *Phys. Rev. Lett.* **57** 245; 1987 High-temperature series expansion for spin glasses. II. Analysis of the series *Phys. Rev.* B **36** 559

[16] Kirkpatrick S, Gelatt C D Jr and Vecchi M P 1983 Optimization by simulated annealing *Science* **220** 671

[17] Omari R, Prejean J J and Souletie J 1984 The extra-dimension $W = kT\ln(t/\tau_0)$ of phase space below the spin glass transition: an experimental study of the relaxation of the magnetization at constant field in CuMn *J. Physique* **45** 1809

[18] De Dominicis C, Kondor I and Temesvari T 1993 Ising spin glass: recent progress in the field theory approach *Int. J. Mod. Phys.* B **7** 986; 1996 Recent advances in the theory of disordered systems: spin glasses, random fields, random polymers *J. Physique* I **6** 21